

Publications

---

9-9-2022

## Height Information Aided 3D Real-Time Large-Scale Underground User Positioning

Houbing Song

*Embry-Riddle Aeronautical University, SONG4@erau.edu*

Chengkai Tang

*Northwestern Polytechnical University*

Cunle Zhang

*Northwestern Polytechnical University*

Lingling Zhang

*Northwestern Polytechnical University*

Yi Zhang

*Northwestern Polytechnical University*

Follow this and additional works at: <https://commons.erau.edu/publication>



Part of the [Computer and Systems Architecture Commons](#), and the [Signal Processing Commons](#)

---


### Scholarly Commons Citation

Song, H., Tang, C., Zhang, C., Zhang, L., & Zhang, Y. (2022). Height Information Aided 3D Real-Time Large-Scale Underground User Positioning. *IET Radar, Sonar & Navigation*, (). <https://doi.org/10.1049/rsn2.12324>

This Article is brought to you for free and open access by Scholarly Commons. It has been accepted for inclusion in Publications by an authorized administrator of Scholarly Commons. For more information, please contact [commons@erau.edu](mailto:commons@erau.edu).

**ORIGINAL RESEARCH**

# Height information aided 3D real-time large-scale underground user positioning

Chengkai Tang<sup>1</sup> | Cunle Zhang<sup>1</sup> | Lingling Zhang<sup>2</sup>  | Yi Zhang<sup>1</sup> | Houbing Song<sup>3</sup><sup>1</sup>School of Electronics and Information, Northwestern Polytechnical University, Xi'an, Shaanxi, China<sup>2</sup>School of Marine Science and Technology, Northwestern Polytechnical University, Xi'an, Shaanxi, China<sup>3</sup>Department of Electrical, Computer, Software, and Systems Engineering, Embry-Riddle Aeronautical University, Daytona Beach, Florida, USA**Correspondence**Lingling Zhang, School of Marine Science and Technology, Northwestern Polytechnical University, Xi'an, Shaanxi, China.  
Email: zhanglingling9999@163.com**Funding information**

National Natural Science Foundation of China, Grant/Award Numbers: 62171735, 62173276, 62101458, 62001392, 61803310, 61801394; Natural Science Basic Research Program of Shaanxi, Grant/Award Numbers: 2022GY-097, 2021JQ-122, 2021JQ-693; China Postdoctoral Science Foundation, Grant/Award Numbers: 2020M673482, 2020M673485

**Abstract**

Due to the cost of inertial navigation and visual navigation equipment and lack of satellite navigation signals, they cannot be used in large-scale underground mining environment. To solve this problem, this study proposes a large-scale underground 3D real-time positioning method with seam height assistance. This method uses the ultra wide band positioning base station as the core and is combined with seam height information to build a factor graph confidence transfer model to realise 3D positioning. The simulation results show that the proposed real-time method is superior to the existing algorithms in positioning accuracy and can meet the needs of large-scale underground users.

## 1 | INTRODUCTION

With the rapid development of global industrialisation and the increasing demand for mineral resources, the mining scale and depth of underground mines have increased significantly, and large and super large mines continue to emerge, resulting in the extremely increased complexity of underground roads. The wide range of underground mining space has led to an increasing demand for the navigation and positioning of personnel and equipment under mines, while traditional satellite navigation technology cannot be used on a large scale under mines due to the weak signals. Therefore, the core foundation of mining is to realise the intelligent automatic navigation and positioning of large-scale mining equipment and personnel in underground mines and build a high-precision real-time three-dimensional positioning system in underground mines [1, 2].

To address the harsh positioning environment of underground mines and solve the problem of large-scale cluster positioning in mines, some scholars have used mature

positioning methods in other fields for mine positioning, mainly inertial navigation positioning and visual navigation positioning, but inertial navigation devices require continuous calibration in use, while visual navigation has high requirements for the stability of light, and the high price also completely restricts the large-scale application of the above devices [3, 4]. Moreover, most of the current underground positioning technologies are based on the mutual independence of positioning targets. There is no communication and positioning topology between users to be located. With the increase in the positioning scale, the amount of positioning calculation and complexity increase exponentially. Another scholar introduced user collaboration theory to try to solve the issue that the above method is only for independent users to deal with large-scale user positioning, but the positioning accuracy and positioning speed are always difficult to reconcile [5, 6]. Therefore, it is urgent to study a large-scale real-time and high-precision user positioning method under mines.

Ultra wide band(UWB) technology has the advantages of low cost, high precision over short distances, low power

This is an open access article under the terms of the Creative Commons Attribution-NonCommercial-NoDerivs License, which permits use and distribution in any medium, provided the original work is properly cited, the use is non-commercial and no modifications or adaptations are made.

© 2022 The Authors. *IET Radar, Sonar & Navigation* published by John Wiley & Sons Ltd on behalf of The Institution of Engineering and Technology.

consumption and suitability for large-scale layouts [7]. Using UWB technology, combined with factor graph theory and auxiliary parameters of the mine height, this paper proposes a three-dimensional real-time positioning method under mines, which provides a new efficient and practical solution for the positioning requirements in large mines.

Under such circumstances, this paper proposes a highly assisted 3D real-time cooperative positioning technology for large-scale clusters in underground mines, solves the problem of cluster positioning, and provides 3D real-time positioning services for large-scale users in underground mines. The probability model of the measurement data of the positioning user in the mine is established by using the UWB signal. Factor graph theory and the confidence transmission criterion are introduced to reduce the calculation overhead of the positioning network and improve the robustness. The factor graph confidence information transmission model is constructed. Combined with the mine height, a large-scale factor graph three-dimensional real-time cooperative positioning algorithm is proposed.

The main contributions of this paper are as follows:

- Combined with the mine environment, the user measurement data model based on UWB is established, and the corresponding mine scene classification and positioning strategy is proposed.
- According to the particularity of the mine environment, the height matching criterion of the mine map is proposed. Combined with factor graph theory and the confidence transfer criterion, a large-scale real-time and high-precision three-dimensional positioning method under mines is proposed.
- A large-scale 3D real-time positioning simulation system in a mine environment is established. The positioning method is verified by semiphysical simulation from three aspects: the number of users, positioning accuracy and real-time, and the effect is good.

The organisational structure of this paper is as follows. The second section introduces the main methods of underground positioning at present. The third section establishes the positioning strategy and model under a mine environment. The fourth section proposes the auxiliary positioning criterion of the mine height and the three-dimensional cooperative positioning method of a large-scale factor graph. The fifth section analyses the performance of the proposed location algorithm through simulation. The sixth section summarises the full text.

## 2 | RELATED WORKS

During the development of the metal mining industry for more than a century, research on cluster user positioning in large-scale underground mines has also made some progress. Satellite navigation can provide precise positioning services outdoors, but in underground mines, satellite signal attenuation is serious, so it is unable to locate mine users effectively [8].

Inertial navigation devices were first used in underground positioning. Inertial measurement units can provide more accurate speed and heading information, but limited by its principle, the error is accumulated at any time, which makes it difficult to apply on a large scale and for a long time [9, 10]. Positioning technology based on visual image matching has relatively considerable positioning accuracy in the shaft but is limited to the coverage of monocular visual image acquisition devices and cannot satisfy the positioning of large-scale mining equipment. The distribution of light sources in the mine has a certain impact on its positioning stability, and its expensive cost also overwhelms underground positioning applications [11]. The underground mine environment is claustrophobic, and light is insufficient. The optical communication method is easily blocked by the equipment and metal ore bed, resulting in communication loss. Under the demand of large-scale positioning, it cannot achieve accurate positioning [12]. Wi-Fi fingerprint matching and positioning can be used for small base users. When facing a large number of mining equipment and staff in a large range, the positioning coverage is limited [13]. Collecting fingerprints from underground locations is inefficient and difficult to expand [14]. UWB technology has considerable precision, simple equipment requirements and strong expansibility, which provides a new idea for underground positioning.

Cooperative theory is usually used in cluster connection topology location, and there are many studies on cooperative location methods. The classical least squares algorithm has a simple principle and low computational complexity. The performance of weighted least squares proposed by Qiu Ran et al. is improved [15], but its accuracy is very limited. Li Jiannan and others proposed the combination of the least square method with Newton iteration, but it still has difficulty meeting the application requirements for the precise positioning of underground mines [16]. The combination of the Kalman filter and optimisation theory can well realise node positioning, but the huge amount of calculations and communication overhead in large mining sites are prohibitive. Huang Yulong's team proposed a variational adaptive Kalman filter algorithm for cooperative positioning [17]. The accuracy was improved, but the speed was not improved. Cui Yuming's team used the extended Kalman filter to enhance the stability of the system [18]. However, the amount of calculation still needs to be considered. The adaptive unscented Kalman filter algorithm proposed by Yin Huajun and others exhibited improvement in the accuracy compared with the traditional Kalman filter [19]. However, the problem of computational complexity has not been solved. Jiang Changhui and others used graphic optimisation method to replace Kalman filter for vector tracking, and realised PDR/GNSS of smart phones through Kalman filter and factor graph optimisation (FGO), but it was still limited by the shortcomings of GNSS and could not be applied in underground mines [20, 21]. The particle filter uses limited particles to draw the distribution curve to deal with a non-linear non-Gaussian environment, but it is often very difficult to draw the distribution curve in a mine environment. Han Yongqiang and others combined a particle filter with track

estimation to improve the robustness of the system [22]. However, this approach creates an additional hardware burden. Bayesian estimation transforms the problem of cooperative location into the problem of variable a posteriori probability distribution and introduces the concepts of factor graph and confidence degree. Qiu Yixi and others introduced confidence into trajectory tracking to realise data fusion, which has considerable complexity, and its accuracy still lags behind that of the Kalman filter method [23]. Tang Chengkai's team proposed the cooperative positioning algorithm of factor graph in three-dimensional space, which realised the three-dimensional application of factor graphs. However, for huge occlusions in a mine environment, the node height is often unavailable, and it is difficult to estimate the coupling error between highly consistent positioning targets, resulting in a high proportion of bad values in the positioning results [24, 25]. The emerging neural network method has improved the accuracy of cooperative positioning, but the training data acquisition and time consumption in underground mines are large problems. In the face of cluster positioning targets, the huge communication overhead makes the positioning lack rapidity and stability, which limits the positioning application of this theory in practical mines. Yuan Lukito et al. proposed a recursive neural network model combined with Wi-Fi to improve the positioning accuracy, but the same shortcomings as Wi-Fi methods exist [26]. Abdullah Cavdar et al. proposed a visible light positioning system based on an artificial neural network, which can be applied to underground space positioning, but there is a large multipath error [27]. Bhagawat Adhikari et al. proposed a neural network positioning model combined with recursive least squares. The model is simple, but the accuracy is limited [28]. Satish R. Jondhale and others proposed a generalised regression neural network model combined with a Kalman filter, which makes up for the lack of accuracy of the Kalman filter, but the amount of calculation is very large [29]. Y. Ansari proposed 3D indoor base on deep convolutional neural network [30]. Zheng Bojun's team proposed using the TensorFlow neural network model for indoor positioning, which has considerable accuracy, but the workload in the early stage is large, which is difficult to apply on a large scale [31].

As a mathematical function decomposition model, factor graph theory and the sum product algorithm have been gradually applied to the field of navigation and positioning in recent years. The GNSS algorithm based on factor graphs has made some progress in satellite navigation [32]. Factor graphs are also used in unmanned vehicle path planning [33]. The application of factor graph models provides a convenient idea for underwater AUV navigation [34]. In terms of wireless location and path planning, innovations on factor graphs are also emerging. For large-scale real-time positioning under complex mines, the application of factor graph theory is still relatively scarce. The mine pipelines are narrow and blocked, the communication between them is limited, and the large rock stratum causes serious shielding and loss, which makes it difficult to realise the high-precision three-dimensional real-time positioning of global cluster users. Therefore, this paper proposes the strategy of overall planning, segmentation

and governance, decomposes the huge underground mine positioning space into a pipeline ad hoc positioning network, uses UWB technology to provide stable communication data, uses a shaft map to assist in matching the user positioning height, and establishes a three-dimensional factor graph real-time cooperative positioning algorithm for large-scale positioning of users in underground mines to obtain three-dimensional accurate and real-time positioning of clustered mining users.

### 3 | UNDERGROUND MINE POSITIONING SCENE MODEL

In this section, we describe the mine positioning scene in a real situation, use UWB to establish the mine pipeline positioning model, and propose the overall positioning and navigation strategy of a large-scale mine.

Modern large-scale mines have a wide range of horizontal and vertical expansion. Considering the underground mine of a large mine as a whole, in addition to the longitudinal deep shaft at the mouth of the mine, it mainly consists of flat and inclined shafts, and the main targeted users in the mine, namely, mining workers and underground mining equipment, are distributed in each flat and inclined shaft. Each mine is connected to each other. There are thick rock strata between the horizontal shaft and the horizontal shaft. There is a large horizontal or vertical sight distance turning and shielding between the horizontal shaft and the inclined shaft, which leads to the loss and attenuation of the wireless communication signal, and it is difficult to realise unified wireless communication in each shaft. The conceptual diagram is shown in Figure 1.

For such a huge positioning scenario, we implement the strategy of overall planning and division and governance. The Cartesian mathematical coordinate system is established based on the mine surface opening so that all underground users are distributed in this coordinate system, and the planning of underground positioning users is consistent on the whole. Considering the well hole distribution and the area where underground positioning users are located, combined with the actual application of wireless communication in the well hole, each well hole is separated according to the connection, and a subcoordinate system is established to solve the problem of large-scale user positioning in the well hole.

In underground mines, shafts bend and cross. In the case of global positioning network, UWB signal attenuation is serious. This non line of sight condition will make UWB module positioning invalid and unable to achieve effective positioning, especially for the third dimension. We can achieve effective two-dimensional positioning in the local positioning network, but we lack height information, so we need to establish a height map to assist positioning, combined with the conversion strategy of local positioning and global positioning, so as to achieve accurate three-dimensional positioning of the global network in large underground mines.

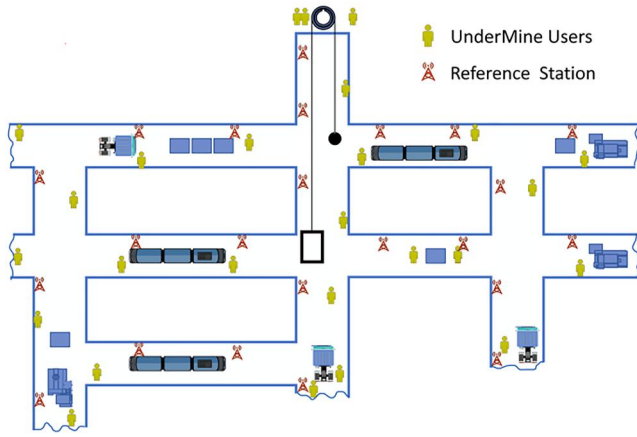


FIGURE 1 Schematic diagram of the mine pipeline positioning scene

## 4 | 3D COOPERATIVE LOCATION ALGORITHM FOR UNDERGROUND USERS

The key point of the positioning service in open underground mines is to satisfy the navigation and positioning of large-scale cluster targets and real-time positioning on the premise of ensuring accuracy. The former requires a high-order positioning solution, and the latter requires a low complexity positioning algorithm. The combination of the two needs to meet the high precision of fixed navigation and the stability of positioning. Based on this, the cooperative positioning theory is introduced, and the factor graph model and confidence transfer algorithm are used to reduce the computational complexity, improve the positioning solution speed, improve the stability of the positioning results and improve the robustness of the positioning system. Combined with the auxiliary matching of the positioning height with the mine map, the three-dimensional real-time cooperative positioning service of the underground mine is achieved.

### 4.1 | Factor graph network cooperative localisation algorithm

In the mine ad hoc network positioning scenario, there are generally two types of underground positioning users: one is the reference base station user whose location is known, and the other is the underground positioning user whose location is to be solved. The coordinates of the positioning user  $i$  under a mine are expressed as  $\mathbf{x}_i = (x_i, y_i)^T$ , where  $x_i$  and  $y_i$  represent the horizontal and vertical coordinates of the underground positioning user respectively. In cooperative positioning, the underground positioning user communicates with the neighbouring user within the communication range and measures the distance, which is represented by  $z_{j \rightarrow i}$ :

$$z_{j \rightarrow i} = \|\mathbf{x}_j - \mathbf{x}_i\| + \xi_{j \rightarrow i} \quad (1)$$

where  $\|\cdot\|$  represents the Euclidean distance and  $\xi_{j \rightarrow i}$  represents the measurement error. Under the condition of sight distance, it follows a Gaussian distribution with a mean of 0 and variance of  $\sigma_{j \rightarrow i}^2$ .

For ease of expression, the following definitions are made:  $S$  represents the set of all reference base station users, and  $M$  represents the set of underground positioning users. For a mine location user  $i$ , the neighbouring reference base station user set is represented by  $S_i$ , and the neighbouring cooperative mine location user set is represented by  $M_i$ . The definition  $Z_i = \{z_{j \rightarrow i} \mid j \in S_i \cup M_i\}$  represents the measured distance and set between underground positioning users  $i$  and neighbouring nodes,  $\mathbf{X} = \{\mathbf{x}_i \mid i \in S\}$  represents the set of user coordinates of all reference base stations, and  $\mathbf{Z} = \{z_i \mid i \in M\}$  represents the set of desired distances measured by all underground positioning users.

According to Bayesian estimation theory, the fundamental purpose is to solve the posterior probability density  $p(\mathbf{x}_i | \mathbf{Z})$  and  $P(y_i | \mathbf{Z})$  of underground positioning user  $i$ , which can be obtained as follows:

$$\begin{aligned} p(\mathbf{X} | \mathbf{Z}) &\propto P(\mathbf{Z} | \mathbf{X}) p(\mathbf{X}) \\ &\propto \prod_{i \in M} \left( \prod_{j \in S_i \cup M_i} p(z_{j \rightarrow i} | x_j, y_j, x_i, y_i) \right) p(x_i) p(y_i) \quad (2) \end{aligned}$$

where  $p(\mathbf{Z} | \mathbf{X})$  represents the joint probability density distribution function,  $p(\mathbf{X})$  represents the joint prior probability density function, and the posterior probability density function is directly proportional to the product of the prior probability density function and the probability density distribution function.  $p(x_i)$  and  $p(y_i)$  are the prior probability distributions of coordinates  $x$  and  $y$ . Defined by the edge probability distribution function, the posterior probability distribution of user  $i$  to be located can be expressed by the edge distribution of Equation (2).

In Equation (2), the product of a series of subfunctions in the form of a joint probability density distribution function easily expresses the function variable relationship by a factor graph, and the variable edge distribution is easily obtained by combining the sum product method. According to the actual positioning scene in the mine, the factor graph structure of the underground positioning users and neighbouring users in the positioning network topology is shown in Figure 2.

Figure 2 is mainly composed of three parts: underground positioning user  $i$ , neighbouring reference base station  $s$  and neighbouring cooperative positioning user  $m$ . For the neighbouring reference base station  $s$  within the communication range, its location coordinates are accurately known, and the information  $x_s$  and  $y_s$  transmitted by the corresponding variable node are constants. At this time, only the likelihood function factor node  $f_{s \rightarrow i}$  and the location coordinate prior distribution factor nodes  $f_{x_s}$  and  $f_{y_s}$  are needed to estimate the coordinates of the underground positioning users. For the neighbouring cooperative positioning user  $m$  within the communication range, the neighbouring underground positioning user and



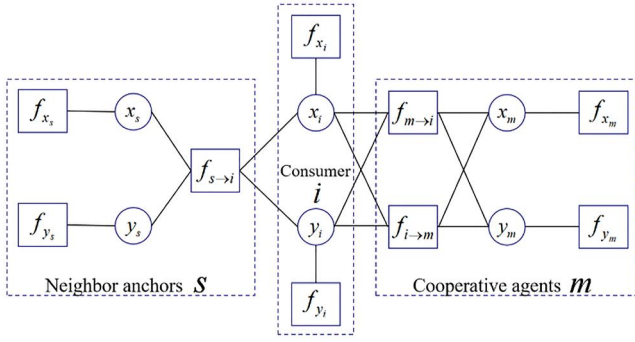


**FIGURE 2** Factor diagram between underground positioning users and neighbouring users in a single well hole

underground positioning user cooperate with each other. The figure presents a symmetrical topology. The factor nodes  $f_{m \rightarrow i}$  and  $f_{i \rightarrow m}$  correspond to the likelihood function, and the factor nodes  $f_{x_i}$ ,  $f_{y_i}$ ,  $f_{x_m}$ , and  $f_{y_m}$  represent the prior probability distribution of the location of users  $i$  and  $m$  to be located. In addition, the corresponding variable nodes are  $x_i$ ,  $y_i$ ,  $x_m$  and  $y_m$ .

Because the relationship between two-point coordinates and the measurement distance between two points is non-linear in practical application, to improve the practicability of the algorithm, combined with the approximate inference theory, the linearised approximation of the measurement information is obtained by using the first-order Taylor series expansion to realise the closed-loop expression of the sum product algorithm. Note here that the measurement information linearisation result of the reference base station between the mine positioning user and the neighbour is  $\hat{d}_{s \rightarrow i}$ , and the measurement information linearisation result of the mine positioning user and the neighbour cooperating with the mine positioning user is  $\hat{d}_{m \rightarrow i}$ .

Before starting the cooperative positioning algorithm, all base stations and underground users in the network are initialised. The reference base station has an accurate position, so its information can be regarded as a Dirac function:

$$\begin{cases} f_{x_s} = \delta(x_s - m_{x_s}) \\ f_{y_s} = \delta(y_s - m_{y_s}) \end{cases} \quad (3)$$

In Equation (3),  $m_{x_s}$  and  $m_{y_s}$  are the abscissa and ordinate information of the reference base station. Let  $m_{x_i}^{(0)}$ ,  $m_{y_i}^{(0)}$ ,  $(\sigma_{x_i}^{(0)})^2$ , and  $(\sigma_{y_i}^{(0)})^2$  be the initial mean and variance information of the user to be located on the horizontal and vertical axes; then, the initialisation of underground positioning user  $i$  can be completed by the following formula:

$$\begin{cases} f_{x_i}(x_i) \propto N\left(m_{x_i}^{(0)}, (\sigma_{x_i}^{(0)})^2\right) \\ f_{y_i}(y_i) \propto N\left(m_{y_i}^{(0)}, (\sigma_{y_i}^{(0)})^2\right) \end{cases} \quad (4)$$

The whole process of realising user location service through the cooperative location algorithm is divided into three steps: calculating the input information, calculating the output

information and updating the probability distribution. Now, we deduce each process in turn, taking iteration  $l$  as an example.

#### 4.1.1 | Calculating the input information

The underground positioning user  $i$  receives the location information  $x_s$  and  $y_s$ , output stream information  $\mu_{x_s \rightarrow f_{s-i}}^{(l-1)}$  and  $\mu_{y_s \rightarrow f_{s-i}}^{(l-1)}$  of its neighbouring reference base station, receives the location estimation information  $\hat{x}_m^{(l-1)}$  and  $\hat{y}_m^{(l-1)}$  and output stream information  $\mu_{x_m \rightarrow f_{m-i}}^{(l-1)}$ ,  $\mu_{y_m \rightarrow f_{m-i}}^{(l-1)}$ ,  $\mu_{x_m \rightarrow f_{i-m}}^{(l-1)}$  and  $\mu_{y_m \rightarrow f_{i-m}}^{(l-1)}$  of its neighbour cooperating with the underground positioning user. The above information is used to calculate the input information at iteration  $l$ : neighbouring reference base station input information stream  $\mu_{f_{s-i} \rightarrow x_i}^{(l)}$  and  $\mu_{f_{s-i} \rightarrow y_i}^{(l)}$ ; neighbour cooperative underground positioning user input information flow  $\mu_{f_{m-i} \rightarrow x_i}^{(l)}$ ,  $\mu_{f_{m-i} \rightarrow y_i}^{(l)}$ ,  $\mu_{f_{i-m} \rightarrow x_i}^{(l)}$  and  $\mu_{f_{i-m} \rightarrow y_i}^{(l)}$ .  $\mu_{f_{s-i} \rightarrow x_i}^{(l)}$  and  $\mu_{f_{m-i} \rightarrow x_i}^{(l)}$  are taken as examples.

a)  $\mu_{f_{s-i} \rightarrow x_i}^{(l)}$ :

The following can be seen from the node representation relationship in the factor diagram:

$$\mu_{f_{s-i} \rightarrow x_i}^{(l)} = \int f_{s-i} \mu_{y_i \rightarrow f_{s-i}}^{(l-1)} dy_i. \quad (5)$$

In Equation (5),  $\mu_{y_i \rightarrow f_{s-i}}^{(l-1)}$  refers to the output flow information of the user's longitudinal axis for underground positioning in the iteration  $l-1$ . Take the abscissa and ordinate  $(\hat{x}_i^{(l-1)}, \hat{y}_i^{(l-1)})$  of the iteration  $l-1$  underground positioning user  $i$ ; the following results are obtained through the known reference base station distribution and the iteration  $l-1$  results:

$$\mu_{f_{s-i} \rightarrow x_i}^{(l)} \propto N\left(m_{x_s} + z_{s-i} \frac{\hat{x}_i^{(l-1)} - m_{x_s}}{\hat{d}_{s-i}^{(l-1)}}, \sigma_{s-i}^2\right). \quad (6)$$

The same can be obtained as follows:

$$\mu_{f_{s-i} \rightarrow y_i}^{(l)} \propto N\left(m_{y_s} + z_{s-i} \frac{\hat{y}_i^{(l-1)} - m_{y_s}}{\hat{d}_{s-i}^{(l-1)}}, \sigma_{s-i}^2\right). \quad (7)$$

b)  $\mu_{f_{m-i} \rightarrow x_i}^{(l)}$ :

The following can be seen from the node representation relationship in the factor diagram:

$$\mu_{f_{m-i} \rightarrow x_i}^{(l)} = \int f_{m-i} \mu_{x_m \rightarrow f_{m-i}}^{(l-1)} \mu_{y_m \rightarrow f_{m-i}}^{(l-1)} \mu_{y_i \rightarrow f_{m-i}}^{(l-1)} dx_m dy_m dy_i. \quad (8)$$

In Equation (8),  $\mu_{x_m \rightarrow f_{m-i}}^{(l-1)}$ ,  $\mu_{y_m \rightarrow f_{m-i}}^{(l-1)}$  and  $\mu_{y_i \rightarrow f_{m-i}}^{(l-1)}$  are the output stream information of the iteration  $l-1$  underground positioning user and obey  $N\left(m_{x_m \rightarrow f_{m-i}}^{(l-1)}, \left(\sigma_{x_m \rightarrow f_{m-i}}^{(l-1)}\right)^2\right)$ ,  $N\left(m_{y_m \rightarrow f_{m-i}}^{(l-1)}, \left(\sigma_{y_m \rightarrow f_{m-i}}^{(l-1)}\right)^2\right)$  and  $N\left(m_{y_i \rightarrow f_{m-i}}^{(l-1)}, \left(\sigma_{y_i \rightarrow f_{m-i}}^{(l-1)}\right)^2\right)$ . The abscissa and ordinate  $\left(\hat{x}_m^{(l-1)}, \hat{y}_m^{(l-1)}\right)$  of the iteration  $l-1$  underground positioning user  $m$  can be obtained as follows:

$$\mu_{f_{m-i} \rightarrow x_i}^{(l)} \propto N\left(m_{x_m \rightarrow f_{m-i}}^{(l-1)} + z_{m \rightarrow i} \frac{\hat{x}_i^{(l-1)} - \hat{x}_m^{(l-1)}}{\hat{d}_{m \rightarrow i}^{(l-1)}}, \sigma_{m \rightarrow i}^2 + \left(\sigma_{x_m \rightarrow f_{m-i}}^{(l-1)}\right)^2\right). \quad (9)$$

The same can be obtained as follows:

$$\mu_{f_{m-i} \rightarrow y_i}^{(l)} \propto N\left(m_{y_m \rightarrow f_{m-i}}^{(l-1)} + z_{m \rightarrow i} \frac{\hat{y}_i^{(l-1)} - \hat{y}_m^{(l-1)}}{\hat{d}_{m \rightarrow i}^{(l-1)}}, \sigma_{m \rightarrow i}^2 + \left(\sigma_{y_m \rightarrow f_{m-i}}^{(l-1)}\right)^2\right). \quad (10)$$

$$\mu_{f_i \rightarrow x_i}^{(l)} \propto N\left(m_{x_m \rightarrow f_{i-m}}^{(l-1)} + z_{i \rightarrow m} \frac{\hat{x}_i^{(l-1)} - \hat{x}_m^{(l-1)}}{\hat{d}_{i \rightarrow m}^{(l-1)}}, \sigma_{i \rightarrow m}^2 + \left(\sigma_{x_m \rightarrow f_{i-m}}^{(l-1)}\right)^2\right). \quad (11)$$

$$\mu_{f_i \rightarrow y_i}^{(l)} \propto N\left(m_{y_m \rightarrow f_{i-m}}^{(l-1)} + z_{i \rightarrow m} \frac{\hat{y}_i^{(l-1)} - \hat{y}_m^{(l-1)}}{\hat{d}_{i \rightarrow m}^{(l-1)}}, \sigma_{i \rightarrow m}^2 + \left(\sigma_{y_m \rightarrow f_{i-m}}^{(l-1)}\right)^2\right). \quad (12)$$

#### 4.1.2 | Calculating the output information

Each underground positioning user calculates the output stream information  $\mu_{x_i \rightarrow f_{s-i}}^{(l)}$ ,  $\mu_{y_i \rightarrow f_{s-i}}^{(l)}$ ,  $\mu_{x_i \rightarrow f_{m-i}}^{(l)}$ ,  $\mu_{y_i \rightarrow f_{m-i}}^{(l)}$ ,  $\mu_{x_i \rightarrow f_{i-m}}^{(l)}$  and  $\mu_{y_i \rightarrow f_{i-m}}^{(l)}$  through the input information calculated in  $a$ . Taking  $\mu_{x_i \rightarrow f_{s-i}}^{(l)}$  as an example, from the sum product method and the factor in Figure 2, the following is obtained:

$$\mu_{x_i \rightarrow f_{s-i}}^{(l)} = f_{x_i} \prod_{j \in \{S_i \setminus s\}} \mu_{f_{j-i} \rightarrow x_i}^{(l)} \prod_{k \in M_i} \mu_{f_{k-i} \rightarrow y_i}^{(l)} \mu_{f_{i-k} \rightarrow y_i}^{(l)}. \quad (13)$$

The mean and variance are calculated as follows:

$$m_{x_i \rightarrow f_{s-i}}^{(l)} = \left(\sigma_{x_i \rightarrow f_{s-i}}^{(l)}\right)^2 \left( \frac{m_{x_i}^{(0)}}{\left(\sigma_{x_i}^{(0)}\right)^2} + \sum_{j \in \{S_i \setminus s\}} \frac{m_{f_{j-i} \rightarrow x_i}^{(l)}}{\left(\sigma_{f_{j-i} \rightarrow x_i}^{(l)}\right)^2} + \sum_{k \in M_i} \left( \frac{m_{f_{k-i} \rightarrow x_i}^{(l)}}{\left(\sigma_{f_{k-i} \rightarrow x_i}^{(l)}\right)^2} + \frac{m_{f_{i-k} \rightarrow x_i}^{(l)}}{\left(\sigma_{f_{i-k} \rightarrow x_i}^{(l)}\right)^2} \right) \right). \quad (14)$$

$$\left(\sigma_{x_i \rightarrow f_{s-i}}^{(l)}\right)^2 = \frac{1}{\left( \frac{1}{\left(\sigma_{x_i}^{(0)}\right)^2} + \sum_{j \in \{S_i \setminus s\}} \frac{1}{\left(\sigma_{f_{j-i} \rightarrow x_i}^{(l)}\right)^2} + \sum_{k \in M_i} \left( \frac{1}{\left(\sigma_{f_{k-i} \rightarrow x_i}^{(l)}\right)^2} + \frac{1}{\left(\sigma_{f_{i-k} \rightarrow x_i}^{(l)}\right)^2} \right) \right)}. \quad (15)$$

#### 4.1.3 | Updating the probability distribution

According to the input information of each function node, the information update formula can be obtained:

$$b_{x_i}^{(l)} = f_{x_i} \prod_{j \in S_i} \mu_{f_{j-i} \rightarrow x_i}^{(l)} \prod_{k \in M_i} \mu_{f_{k-i} \rightarrow x_i}^{(l)} \mu_{f_{i-k} \rightarrow x_i}^{(l)}. \quad (16)$$

$$b_{y_i}^{(l)} = f_{y_i} \prod_{j \in S_i} \mu_{f_{j-i} \rightarrow y_i}^{(l)} \prod_{k \in M_i} \mu_{f_{k-i} \rightarrow y_i}^{(l)} \mu_{f_{i-k} \rightarrow y_i}^{(l)}. \quad (17)$$

The mean and variance can be obtained by substitution:

$$m_{x_i}^{(l)} = \left(\sigma_{x_i}^{(l)}\right)^2 \left( \frac{m_{x_i}^{(0)}}{\left(\sigma_{x_i}^{(0)}\right)^2} + \sum_{j \in S_i} \frac{m_{f_{j-i} \rightarrow x_i}^{(l)}}{\left(\sigma_{f_{j-i} \rightarrow x_i}^{(l)}\right)^2} + \sum_{k \in M_i} \left( \frac{m_{f_{k-i} \rightarrow x_i}^{(l)}}{\left(\sigma_{f_{k-i} \rightarrow x_i}^{(l)}\right)^2} + \frac{m_{f_{i-k} \rightarrow x_i}^{(l)}}{\left(\sigma_{f_{i-k} \rightarrow x_i}^{(l)}\right)^2} \right) \right). \quad (18)$$

$$\left(\sigma_{x_i}^{(l)}\right)^2 = \frac{1}{\left( \frac{1}{\left(\sigma_{x_i}^{(0)}\right)^2} + \sum_{j \in S_i} \frac{1}{\left(\sigma_{f_{j-i} \rightarrow x_i}^{(l)}\right)^2} + \sum_{k \in M_i} \left( \frac{1}{\left(\sigma_{f_{k-i} \rightarrow x_i}^{(l)}\right)^2} + \frac{1}{\left(\sigma_{f_{i-k} \rightarrow x_i}^{(l)}\right)^2} \right) \right)}. \quad (19)$$

$$m_{y_i}^{(l)} = \left(\sigma_{y_i}^{(l)}\right)^2 \left( \frac{m_{y_i}^{(0)}}{\left(\sigma_{y_i}^{(0)}\right)^2} + \sum_{j \in S_i} \frac{m_{f_{j-i} \rightarrow y_i}^{(l)}}{\left(\sigma_{f_{j-i} \rightarrow y_i}^{(l)}\right)^2} + \sum_{k \in M_i} \left( \frac{m_{f_{k-i} \rightarrow y_i}^{(l)}}{\left(\sigma_{f_{k-i} \rightarrow y_i}^{(l)}\right)^2} + \frac{m_{f_{i-k} \rightarrow y_i}^{(l)}}{\left(\sigma_{f_{i-k} \rightarrow y_i}^{(l)}\right)^2} \right) \right). \quad (20)$$

$$\begin{aligned} & \left( \sigma_{y_i}^{(l)} \right)^2 \\ &= \frac{1}{\left( \left( \sigma_{y_i}^{(0)} \right)^2 + \sum_{j \in S_i} \frac{1}{\left( \sigma_{j \rightarrow i}^{(l)} \right)^2} + \sum_{k \in M_i} \left( \frac{1}{\left( \sigma_{k \rightarrow i}^{(l)} \right)^2} + \frac{1}{\left( \sigma_{j_i \rightarrow k}^{(l)} \right)^2} \right) \right)} \end{aligned} \quad \begin{cases} \omega_\xi = \frac{L_\xi}{L_\xi + L_\zeta} \\ \omega_\zeta = \frac{L_\zeta}{L_\xi + L_\zeta} \end{cases} \quad (23)$$

When all underground positioning users complete the algorithm operation and the  $x_i$  and  $y_i$  information of the variable node converges or reaches the maximum number of iterations, the location update is completed to obtain the final positioning result.

## 4.2 | Underground map height matching

Restricted by the narrow and long positioning space of the underground shaft, the span of the reference base station in the vertical direction is limited, and considering the multipath loss of UWB signal propagation, it often leads to the loss of the accuracy of the third dimension. Therefore, this paper proposes a method to match the third dimension by using the arithmetic average of the height weight of the shaft map. In the process of mining underground mineral resources, shafts such as shafts and inclined shafts are formed by mechanical mining, and the shaft height is calibrated at the same time of mining. All shaft height data are uniformly managed by mining personnel in the database. Before the underground mine establishes the positioning network, bind the geographical height of the shaft when deploying the reference base station to obtain the height map to provide matching for the global three-dimensional positioning. To illustrate the problem,  $(x_q, y_q, z_q)$  is used to represent the coordinates of the underground positioning user  $q$ , and  $(X_p, Y_p, Z_p)$  is used to represent the coordinate value of the reference base station  $p$ . The distance between the underground positioning user  $q$  and the reference base station  $p$  measured by the UWB signal is  $L_{p,q}$ ; then, the distance from the underground positioning user  $q$  to all the reference base stations is aggregated into  $L = \{L_{0,q}, L_{1,q}, \dots, L_{p,q}, \dots, L_{S,q}\}$ . According to optimisation theory, among many reference base stations, we can always find two reference base stations with the smallest distance from the underground positioning user. In the mine structure, these two reference base stations have the greatest impact on the third dimension of the underground positioning user. Let  $L_\xi$  be the largest element in  $L$  and  $L_\zeta$  be the second largest element in  $L$ ; then, the following formula is obtained:

$$\begin{cases} L_\xi = \max\{L_{0,q}, L_{1,q}, \dots, L_{p,q}, \dots, L_{S,q}\} \\ L_\zeta = \max_{p \neq \xi} \{L_{0,q}, L_{1,q}, \dots, L_{p,q}, \dots, L_{S,q}\} \end{cases} \quad (22)$$

The influence weights of  $L_\xi$  and  $L_\zeta$  on the positioning users under the mine are  $\omega_\xi$  and  $\omega_\zeta$ :

If the coordinate of the largest element in the reference base station is  $(X_\xi, Y_\xi, Z_\xi)$  and the coordinate of the second largest element is  $(X_\zeta, Y_\zeta, Z_\zeta)$ , the third dimension  $z_q$  of the underground positioning user coordinate  $(x_q, y_q, z_q)$  can be defined by the following formula:

$$z_q = \omega_\xi Z_\xi + \omega_\zeta Z_\zeta. \quad (24)$$

Thus far, we have completed the three-dimensional cooperative positioning combined with auxiliary matching of the underground mine map height.

The flow of the 3D real-time positioning method under a large-scale mine based on height assistance proposed in this paper is shown in Figure 3.

## 5 | ALGORITHM SIMULATION AND ANALYSIS

To verify the outstanding performance of the algorithm proposed in this paper, this section analyses and explains it through a series of simulation comparisons. Through simulation, we compare the positioning conditions of several positioning methods in the shaft positioning environment proposed in this paper, in which we focus on the user scale, real-time positioning, positioning accuracy and stability of underground positioning.

In this part, our algorithm simulation is based on the following preconditions:

- The simulation area is set as a  $1 \times 10 \times 10$  km cube mine, and three single shaft local positioning networks are set inside.
- There is one positioning network reference base station per kilometre per layer, and the spatial distribution structure adopts random network topology rather than standardised geometric topology.
- The UWB ranging error in all positioning algorithms is consistent and set to 0.1 m.
- Ranging data measurement synchronisation and transmission synchronisation are implemented in each algorithm.
- In this paper, the number of localisation iterations in the algorithm and neural network is set to 30.

### 5.1 | Analysis of the convergence rate of the positioning error of underground personnel

The simulation takes the root mean square error (RMSE) as the evaluation index and considers the positioning when the number of users under the mine is 100, 500 and 1000. The



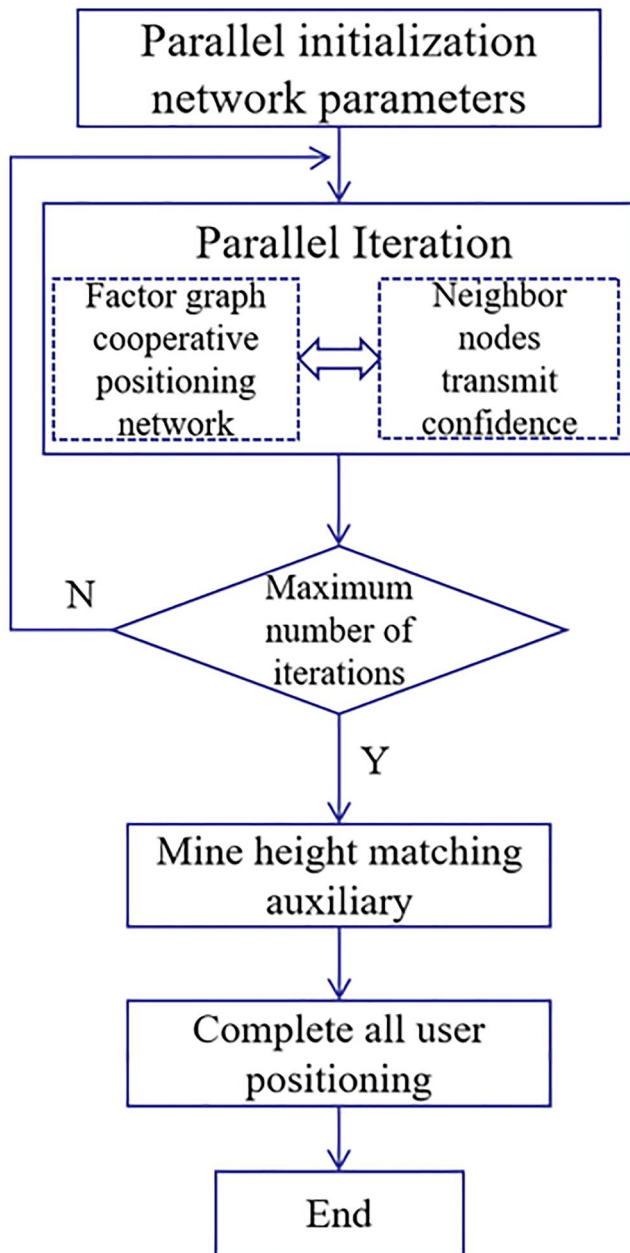


**FIGURE 3** Flow chart of the 3D real-time positioning algorithm for large-scale underground users based on height assistance

simulation is also compared with the weighted least squares method (WLS) [15], the factor graph three-dimensional colocation method (3DFG) [23] and the generalised regression neural network method (GRNN) [29].

Figure 4 shows the root mean square error in the overall space of the four algorithms when the number of underground users is 100, Figure 5 shows the root mean square error in the overall space of the four algorithms when the number of underground users is 500, and Figure 6 shows the root mean square error in the overall space of the four algorithms when the number of underground users is 1000. It can be seen that when the number of users under the mine is 100, the final error of the algorithm proposed in this paper is maintained at

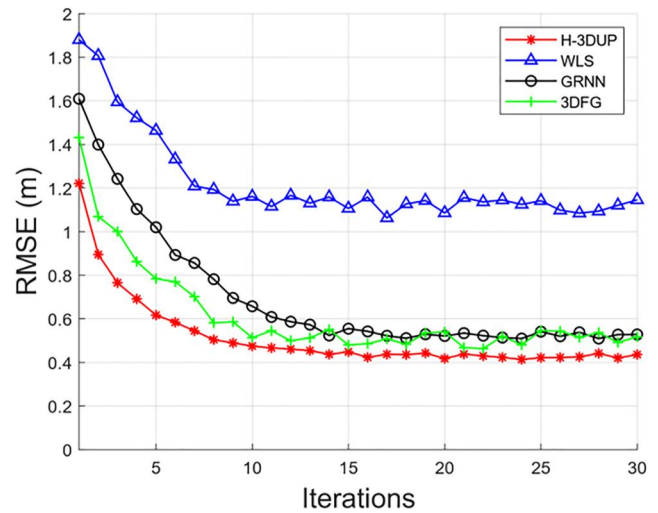


**FIGURE 4** Overall positioning error when the number of underground users is 100

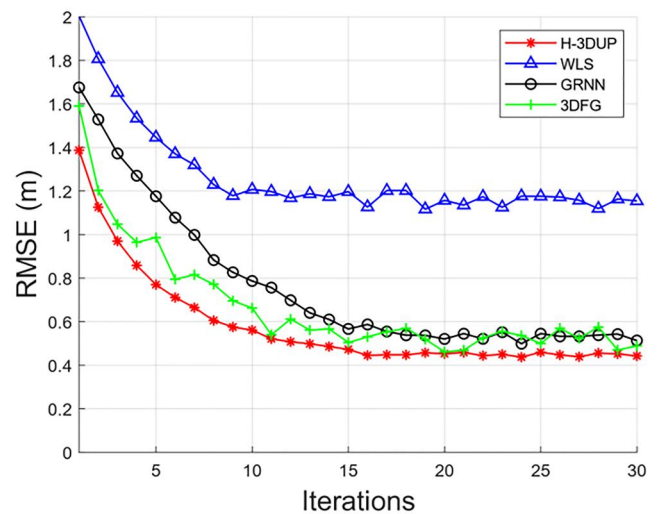


**FIGURE 5** Overall positioning error when the number of underground users is 500

approximately 0.42, 0.7 m higher than that of WLS and 0.1 m higher than that of 3DFG and GRNN, but the error convergence speed is faster than both, and the convergence result is more stable. When the number of users under the mine is 500, the final error of the algorithm proposed in this paper is maintained at approximately 0.44 m, which is approximately 0.7 m higher than that of WLS and approximately 0.1 m higher than that of 3DFG and GRNN. The convergence speed is obviously better than that of GRNN, and the stability of the result is obvious. When the number of users under the mine is 1000, the final error of the algorithm proposed in this paper is maintained at approximately 0.44 m, which is still approximately 0.7 m higher than that of WLS and approximately 0.1 m higher than that of 3DFG and GRNN, and the convergence is only half of that of GRNN. Comparing the positioning mean square error diagrams of two different numbers of underground positioning users, it can be seen that when the

positioning scale is expanded, the positioning accuracy of the algorithm proposed in this paper has almost no loss, the positioning speed is still considerable, and the stability of the positioning results is excellent, which is fully applicable to the underground real-time positioning of large-scale positioning users.

## 5.2 | Accuracy and real-time analysis of underground positioning

The simulation here still takes the root mean square error (RMSE) as the evaluation index and considers the positioning situation when the number of underground positioning users is 1000. The simulation is also compared with the weighted least squares method (WLS) [15], the factor graph three-dimensional colocation method (3DFG) [23] and the generalised regression neural network method (GRNN) [29].

Figure 7 shows the root mean square error of the four algorithms in the respective directions of the three-dimensional coordinate axis when the number of users under the mine is 1000. It can be seen that when the number of users under the mine is 1000, the positioning accuracy of the algorithm proposed in this paper is finally maintained at 0.3 m in three dimensions, which is 0.5, 0.1 and 0.1 m higher than that of WLS, GRNN and 3DFG, respectively, especially in the third dimension. At the same time, the convergence of the results is achieved only in 5–10 iterations, and its positioning speed is also the fastest among the four algorithms. Through comparative analysis, it can be found that in the case of cluster positioning users, the accuracy of the positioning algorithm proposed in this paper is still guaranteed, and the positioning speed and positioning accuracy are significantly better than those of the other two algorithms, which realises three-dimensional real-time positioning of large-scale users in underground mines.

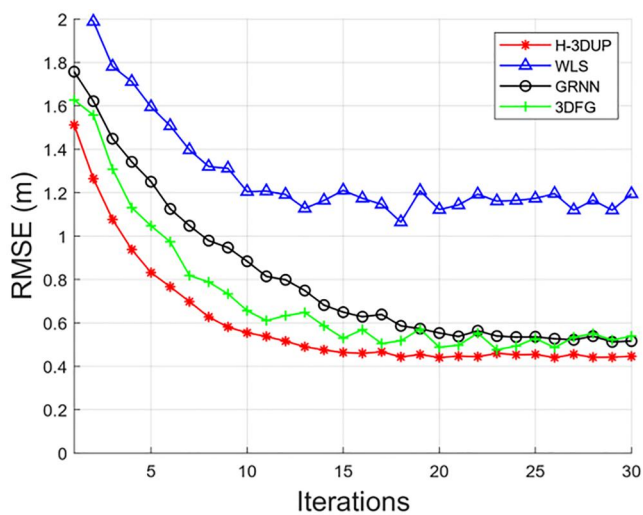


**FIGURE 6** Overall positioning error when the number of underground users is 1000

## 5.3 | Signal mutation error analysis

In this part, the root mean square error (RMSE) is still taken as the evaluation index, and the dynamic positioning of different positioning time slots after the UWB signal is blocked is considered when the number of underground positioning users distributed in a mine pipeline is 500.

Figure 8 shows the root mean square error of the four algorithms on the spatial three-dimensional coordinate axis when the UWB signal is blocked and the number of underground positioning users distributed in a mine pipeline is 500. At the sixth iteration point, some UWB signals are blocked, and the positioning results are abrupt due to the increase in the measurement information error of some positioning users. The positioning results of the four algorithms are greatly affected. The WLS results fluctuate greatly and become stable after the

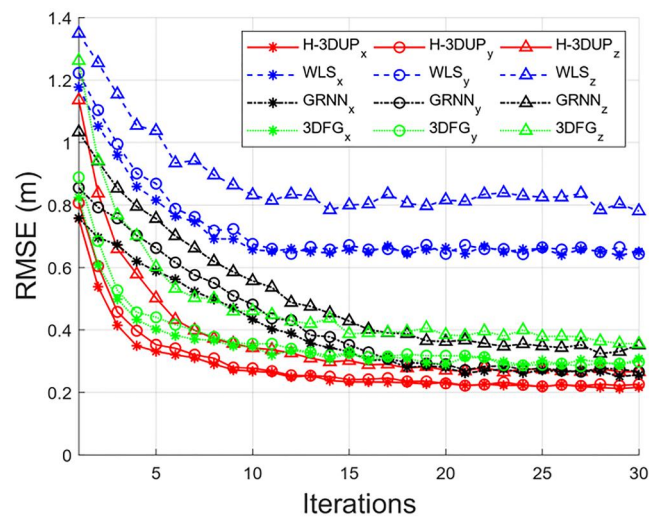


**FIGURE 7** Errors of the four positioning algorithms on the three coordinate axes

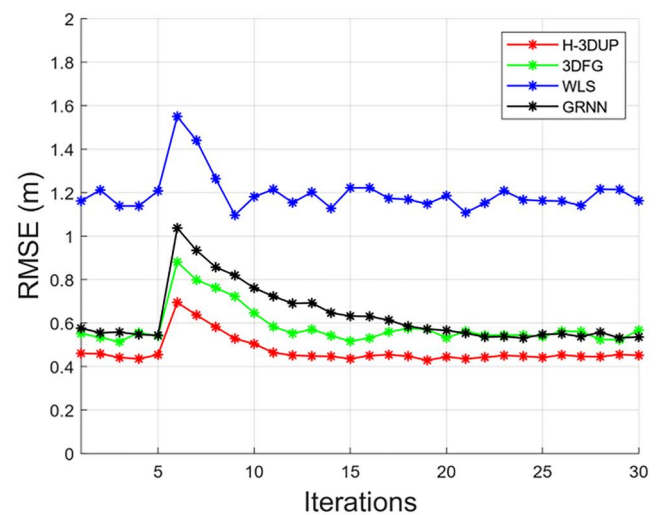


**FIGURE 8** Root mean square error (RMSE) of the three algorithms in different time slots during signal occlusion

signal occlusion disappears, but the overall error is large. The GRNN error increases rapidly, and it still has a great impact on the subsequent positioning after the occlusion disappears; it gradually becomes stable after multiple iterations. The 3DFG error also becomes stable after increasing, but the stability and accuracy of the results are still poor. The mutation error of the algorithm in this paper is small, and it converges and degrades quickly in finite iterations, which shows that the algorithm has good positioning stability and is very suitable for the positioning service demand of stable positioning in underground mines.

Through the simulation comparison under different conditions, we find that the algorithm proposed in this paper is suitable for large-scale cluster user positioning in underground mines, can provide high-precision fast three-dimensional real-time cooperative positioning, and meets the requirements of stable and accurate positioning in complex underground mines.

## 6 | CONCLUSION

Based on a modern large-scale underground mine environment, aiming at the rapid, accurate and stable positioning needs of underground users, this paper proposes a three-dimensional real-time positioning method under large-scale mines based on high assistance. Through the simulation of underground positioning user scale, positioning accuracy and stability and signal mutation error analysis, the positioning performance of this method is relatively better when the number of positioning users is large, and the accuracy is 60% higher than that of WLS. The result convergence is realised at only half the iteration times of GRNN, and the error correction is realised at only 5 times of iteration when the signal mutates, which demonstrates strong robustness. In the positioning scene of complex claustrophobic mine pipelines in large mines, facing a large number of underground users, the positioning algorithm proposed in this paper has great advantages and practicability in the positioning scale, positioning accuracy, positioning speed and positioning stability.

## ACKNOWLEDGEMENTS

The authors thank the editors for rigorous work and the anonymous reviewers for their comments and suggestions. This work was supported in part by the National Natural Science Foundation of China under Grant 62171735, 62173276, 62101458, 62001392, 61803310 and 61801394, in part by the Natural Science Basic Research Program of Shaanxi under Grant 2022GY-097, 2021JQ-122 and 2021JQ-693, and in part by the China Postdoctoral Science Foundation under Grant 2020M673482 and 2020M673485.

## CONFLICT OF INTEREST

The authors declare that there is no conflict of interest.

## DATA AVAILABILITY STATEMENT

Research data are not shared.

## ORCID

Lingling Zhang  <https://orcid.org/0000-0002-9834-7410>

## REFERENCES

- Schneider, O.: Requirements for positioning and navigation in underground constructions. In: 2010 International Conference on Indoor Positioning and Indoor Navigation, pp. 1–4 (2010)
- Ranjan, A., et al.: Opportunities and challenges in health sensing for extreme industrial environment: perspectives from underground mines. *IEEE Access*. 7, 139.181–139.195 (2019). <https://doi.org/10.1109/access.2019.2941436>
- Dunn, M.T., et al.: High accuracy inertial navigation for underground mining machinery. In: 2012 IEEE International Conference on Automation Science and Engineering (CASE), pp. 1179–1183 (2012)
- Li, M., et al.: Efficient laser-based 3D SLAM for coal mine rescue robots. *IEEE Access*. 7, 14124–14138 (2019). <https://doi.org/10.1109/access.2018.2889304>
- Luo, C., et al.: Shearer positioning for mining fleet cooperative movement in GPS-denied environments. In: 2016 IEEE Chinese Guidance, Navigation and Control Conference (CGNCC), pp. 503–506 (2016)
- Dayekh, S., et al.: Cooperative geo-location in underground mines: a novel fingerprint positioning technique exploiting spatio-temporal diversity. In: 2011 IEEE 22nd International Symposium on Personal, Indoor and Mobile Radio Communications, pp. 1319–1324 (2011)
- Blazek, J., Jiranek, J., Bajar, J.: Indoor passive positioning technique using ultra wide band modules. In: 2019 International Conference on Military Technologies (ICMT), pp. 1–5 (2019)
- Zhang, B., et al.: Research on mine robot positioning based on weighted centroid method. In: 2018 International Conference on Robots & Intelligent System (ICRIS), pp. 17–20 (2018)
- Yang, H., et al.: A stable SINS/UWB integrated positioning method of shearer based on the multi-model intelligent switching algorithm. *IEEE Access*. 7, 29128–29138 (2019). <https://doi.org/10.1109/access.2019.2898212>
- Wu, F., Liu, Z.: Research on UWB/IMU fusion positioning technology in mine. In: 2020 International Conference on Intelligent Transportation Big Data & Smart City (ICITBS), pp. 934–937 (2020)
- Huang, J., et al.: Stereo matching algorithm for autonomous positioning of underground mine robots. In: 2018 International Conference on Robots & Intelligent System (ICRIS), pp. 40–43 (2018)
- Pang, M., et al.: Achieving reliable underground positioning with visible light. *IEEE Trans. Instrum. Meas.* 71, 1–15 (2022). <https://doi.org/10.1109/tim.2022.3159975>
- Joseph, R., Sasi, S.B.: Indoor positioning using WiFi fingerprint. In: 2018 International Conference on Circuits and Systems in Digital Enterprise Technology (ICCSDET), pp. 1–3 (2018)
- Zhao, Y., et al.: System performance analysis of multi-user single-node indoor positioning. In: 2019 Computing, Communications and IoT Applications (ComComAp), pp. 123–128 (2019)
- Ran, Q., et al.: A weighted least squares source localization algorithm using TDOA measurements in wireless sensor networks. In: 2016 6th International Conference on Electronics Information and Emergency Communication (ICEIEC), pp. 10–13 (2016)
- Li, J., Sun, B.: Hybrid algorithm based on Newton iteration and least square method for sound source positioning. In: 2020 IEEE 5th International Conference on Signal and Image Processing (ICSIP), pp. 557–561 (2020)
- Huang, Y., et al.: An improved variational adaptive Kalman filter for cooperative localization. *IEEE Sensor. J.* 21(9), 10775–10786 (2021). <https://doi.org/10.1109/jsen.2021.3056207>
- Cui, Y., et al.: Integrated positioning system of unmanned automatic vehicle in coal mines. *IEEE Trans. Instrum. Meas.* 70, 1–13 (2021). <https://doi.org/10.1109/tim.2021.3083903>
- Yin, H., et al.: A positioning algorithm based on improved adaptive unscented Kalman filter. In: 2020 12th International Conference on Intelligent Human-Machine Systems and Cybernetics (IHMSC), pp. 171–174 (2020)

20. Jiang, C., et al.: GNSS vector tracking method using graph optimization. *IEEE Trans. Circuits Syst. II: Express Br* 68(4), 1313–1317 (2020). <https://doi.org/10.1109/tcsii.2020.3025455>
21. Jiang, C., et al.: Implementation and performance analysis of the PDR/GNSS integration on a smartphone. *GPS Solut.* 26(3), 1–9 (2022). <https://doi.org/10.1007/s10291-022-01260-0>
22. Han, Y., et al.: A multi - platform cooperative localization method based on dead reckoning and particle filtering. In: 2019 Chinese Control Conference (CCC), pp. 4037–4041 (2019)
23. Tang, C., et al.: Geometric-manifold-assisted distributed navigation probabilistic information fusion cooperative positioning algorithm. *Rem. Sens.* 13(24), 4987–5007 (2021). <https://doi.org/10.3390/rs13244987>
24. Chiou, Y., Tsai, F.: A reduced-complexity data-fusion algorithm using belief propagation for location tracking in heterogeneous observations. *IEEE Trans. Cybern.* 44(6), 922–935 (2014). <https://doi.org/10.1109/tyb.2013.2276749>
25. Zhu, X., et al.: Weighted factor graph aided distributed cooperative position algorithm. In: 2019 IEEE International Conference on Signal Processing, Communications and Computing (ICSPCC), pp. 1–5 (2019)
26. Lukito, Y., Chrismanto, A.R.: Recurrent neural networks model for WiFi-based indoor positioning system. In: 2017 International Conference on Smart Cities, Automation & Intelligent Computing Systems (ICONSONICS), pp. 121–125 (2017)
27. Cavdar, A., Türk, K.: Artificial neural network based indoor positioning in visible light communication systems. In: 2018 International Conference on Artificial Intelligence and Data Processing (IDAP), pp. 1–7 (2018)
28. Adhikari, B., Fernando, X.N.: A neural network based recursive least square multilateration technique for indoor positioning. In: 2021 IEEE 26th International Workshop on Computer Aided Modeling and Design of Communication Links and Networks (CAMAD), pp. 1–6 (2021)
29. Jondhale, S.R., Deshpande, R.S.: Kalman filtering framework-based real time target tracking in wireless sensor networks using generalized regression neural networks. *IEEE Sensor. J.* 19(1), 224–233 (2019). <https://doi.org/10.1109/jsen.2018.2873357>
30. Ansari, Y., et al.: Prediction of indoor wireless coverage from 3D floor plans using deep convolutional neural networks. In: 2021 IEEE 46th Conference on Local Computer Networks (LCN), pp. 435–438 (2021)
31. Zheng, B., Masuda, T., Shibata, T.: An indoor positioning with a neural network model of TensorFlow for machine learning. In: 2021 International Symposium on Intelligent Signal Processing and Communication Systems (ISPACS), pp. 1–2 (2021)
32. Wen, W., Hsu, L.-T.: Towards robust GNSS positioning and real-time kinematic using factor graph optimization. In: 2021 IEEE International Conference on Robotics and Automation (ICRA), pp. 5884–5890 (2021)
33. Chen, H., Tang, C., Li, Y.: Unmanned vehicle positioning method in satellite-jamming environment based on improved factor graph. In: 2020 IEEE 3rd International Conference on Electronic Information and Communication Technology (ICEICT), pp. 383–387 (2020)
34. Si, S., et al.: A new underwater all source positioning and navigation (ASPN) algorithm based on factor graph. In: 2019 Chinese Control and Decision Conference (CCDC), pp. 2742–2746 (2019)

**How to cite this article:** Tang, C., et al.: Height information aided 3D real-time large-scale underground user positioning. *IET Radar Sonar Navig.* 1–11 (2022). <https://doi.org/10.1049/rsn2.12324>